On the photobehaviour of curcumin in biocompatible hosts: The role of H-abstraction in the photodegradation and photosensitization

Francesca Laneri [a], Claudia Conte [b], Cristina Parisi [a], Ovidio Catanzano [b], Aurore Fraix [a,*], Fabiana Quaglia [b], Salvatore Sortino [a]

[a] PhotoChemLab, Department of Drug and Health Sciences, University of Catania, I-95125 Catania, Italy

[b] Drug Delivery Laboratory, Department of Pharmacy, University of Napoli Federico II, I-80131 Napoli, Italy

Abstract

Curcumin (CUR) is a naturally occurring pigment extensively studied due to its therapeutic activity and delivered by suitable nanocarriers to overcome poor solubility in aqueous media. The significant absorption of CUR in the visible blue region has prompted its use as a potential phototherapeutic agent in treating infectious and cancer diseases, although the mechanism underlying the phototoxic effects is still not fully understood. This contri- bution investigates the photobehaviour of CUR within polymeric micelles, microemulsions, and zein nano- particles, chosen as biocompatible nanocarriers, and human serum albumin as a representative biomolecule. Spectroscopic studies indicate that in all host systems, the enolic tautomeric form of CUR is converted in a significant amount of the diketo form because of the perturbation of the intramolecular hydrogen bond. This leads to intermolecular H-abstraction from the host components by the lowest excited triplet state of CUR with the formation of the corresponding ketyl radical, detected by nanosecond laser flash photolysis. This radical is oxidized by molecular oxygen, likely generating peroxyl and hydroperoxyl radical species, unless in Zein, reasonably due to the poor availability of oxygen in the closely packed structure of this nanocarrier. In

contrast, no detectable formation of singlet oxygen was revealed in all the systems. Overall these results highlight the key role of the H-abstraction process over singlet oxygen sensitization as a primary photochemical pathway strictly dictated by the specific features of the microenvironment, providing new insights into the photoreactivity of CUR in biocompatible hosts that can also be useful for a better understanding of its phototoxicity mechanism.

Keywords

Curcumin Light

Hydrogen abstraction Drug delivery systems

1. Introduction

Curcumin (CUR), 1,7-bis(4-hydroxy-3-methoxyphenyl)-1,6-epta- diene-3,5-dione, is a yellow-orange pigment obtained from the rhizome of *Curcuma longa* [1] and object massive interest among the scientific community owing to its wide variety of medicinal properties. CUR has been shown to possess anticancer [2], antioxidant [3], and wound healing [4] properties, as well as beneficial effects in cardio- vascular [5] and neurodegenerative diseases [6].

One of the most extensively studied effects of CUR is related to its interaction with visible light due to its intense absorption in the blue region. In this regard, CUR has been extensively proposed as a suitable photosensitizer (PS) for photodynamic therapy (PDT) [7–9]. PDT is a promising unconventional treatment for cancer and bacterial diseases mainly based on the light-induced generation of highly reactive singlet oxygen ($^1O_2$) [10,11]. This species is produced catalytically by a collisional energy transfer process between the excited triplet state of a suitable PS and the nearby molecular oxygen and is accepted to be the main mediator of cytotoxic reactions in PDT treatments [12,13]. Be- sides, a less efficient electron transfer process between the PS and molecular oxygen may lead to the formation of superoxide anion ($O^{\bullet}$), which eventually generates other and more cytotoxic reactive oxygen species (ROS) such as H_2O_2 and $^{\bullet}OH$. However, phototoxic effects in- dependent of the presence of oxygen have also been proposed [14].

Although extensive literature data report light-induced biological effects of CUR in many systems, they are not often accompanied by as much data on convincing evidence regarding the main species respon- sible for these photoinduced phenomena. This aspect is quite surprising, taking into account that several studies carried out in organic solvents and micellar systems have highlighted well that the photophysical and photochemical properties of CUR are very sensitive to both the features of the microenvironment (polarity, H-bond, H-donating capability, *etc.*) [14–21] and the dominance of either the enolic or diketo form of its tautomeric equilibrium [22] (Scheme 1).

CUR is practically insoluble in water media, and therefore its de- livery *via* lipidic or polymeric vehicles as liposomes, nanoparticles, mi- crospheres, microemulsions, solid dispersions, and dendrimers has been attempted to increase CUR bioavailability [23–25]. These approaches, of course, focus on the technological properties of CUR vehicles but do not consider the fate of CUR upon light irradiation.

Therefore, additional efforts to investigate the photochemical properties of CUR in different host microenvironments can be useful not only for a better under- standing of its photobehaviour in drug-delivery systems but also for gaining useful insights into the mechanisms involved in the photobiological effects. To this end, in this paper, we report a spectroscopic and photochemical investigation on CUR formulated in Pluronic® polymeric micelles, microemulsions, and zein nanoparticles (NPs), chosen as biocompatible nanocarriers (Scheme 2), human serum albumin (HSA) as representative biomolecule and, for the sake of comparison, also in dioxane and ethanol, chosen as representative solvents with different features.

2. Results and discussion

2.1. Spectroscopic Properties and Steady-State Photolysis of CUR in the Host Systems

Mixed micelles of Pluronic®, an oil/water (o/w) microemulsion, and nanoparticles (NPs) of Zein have been selected as representative nano- carriers able to incorporate lipophilic molecules with diverse structural characteristics. Pluronic® micelles are supramolecular structures with a hydrophobic core of polypropylene oxide able to host hydrophobic molecules and a surrounding shell of polyoxyethylene. Micelles pre- pared by a mixture of Pluronic F127 and P123 are less prone to disso- ciation in unimers upon dilution in aqueous media due to a lower critical micelle concentration than the single components [26]. The micro- emulsion formulation contains Labrasol® and Lauroglycol® FCC, two lipophilic components with well-known biocompatibility and surfactant properties able to act as a solubilizer for poorly soluble molecules. The w/o microemulsion is spontaneously formed under low mixing rates from Labrasol®/Lauroglycol® FCC mixture and water at appropriate ratios. The lipophilic components allow the solubilization of lipophilic compounds that remain mainly confined in the oily phase. Both pluronic micelles and microemulsions share the common feature of being trans- parent to light [26,27] and have been proposed as nanocarriers suitable for PDT with CUR [26,27]. Zein, a hydrophobic protein soluble in vol- atile organic solvents, gives colloidal dispersions of NPs with a typical positive surface due to the presence of glutamine loops in the primary protein structure. Zein NPs incorporate lipophilic molecules in the hy-

drophobic pockets, can be diluted in water, and scatter visible light as a function of their size, like many other polymeric NPs.

Table 1 reports the properties of the different biocompatible nanocarriers with CUR. The amount of CUR in the Pluronic® micelles and the microemulsion was adjusted to allow photophysical characterization, thus avoiding any sample dilution that could alter the structure of the nanocarriers and promote CUR precipitation. All the steps were carried out by protecting the sample from the environmental light. Pluronic® micelles prepared by the thin-film hy- dration incorporate CUR quantitatively, are small with low poly- dispersity, and are transparent to light. The composition of the prototype microemulsion containing Labrasol®:Lauroglycol® FCC: water at 20:2.5:77.5 v/v/v was based on the pseudo-ternary phase di- agrams described previously [28], and the solubility of CUR in the oily phase. Remarkably, the microemulsion allowed the dissolution of CUR up to 1 mg/mL due to the solubility enhancer activity of the oily components. The microemulsion is formed by tiny particles with a narrow size distribution and a slightly negative Z potential (ζ) and is transparent to light. Zein NPs show a larger D_H with a low polydispersity and a positive ζ due to glutamine loops on the NP surface. The encapsulation efficiency of CUR in NPs was almost complete and the sample could be diluted in water without any change of size (data not shown).

As anticipated in the introduction, CUR may exist in two tautomeric forms whose abundance is strictly dependent on both microenvironment polarity and H-bond capability. Fig. 1A shows the normalized UV–Vis absorption spectra of CUR encapsulated within Pluronic® polymeric micelles, an o/w microemulsion, and Zein NPs, associated with HSA and, for the sake of comparison solubilized in dioxane and ethanol. In dioxane, a solvent with no H-bonding capability, the main absorption band of CUR is well structured and shows a maximum at 420 nm and two shoulders at 400 and 440 nm, respectively. According to the literature [15–18], these spectral features are similar to those observed in other aprotic solvents and are due to the exclusive presence of the enolic form of CUR in the ground state. In ethanol, a more polar solvent with H- bonding capability, the absorption loses the vibronic structure, broadens, and significantly shifts to the red. This behaviour results from intermolecular H-bonds with the solvent, which prevail on the intra- molecular one, shifting the equilibrium of Scheme 1 towards the diketo form [15–18].

The absorption spectra of CUR observed in the presence of Pluronic® micelles and the microemulsion are characterized by a significant broadening and a red shift

compared to dioxane but still exhibit some vibronic structure which, in contrast, is almost completely lost when CUR is encapsulated within zein NPs and HSA and is accompanied by an absorption extending beyond 500 nm.

The normalized fluorescence emission spectra of CUR are reported in Fig. 1B. Analogously to the absorption, the spectrum in dioxane shows a vibrational structure that is lost in ethanol, where the emission band is also significantly broadened and red-shifted. The fluorescence in the Pluronic® micelles and the microemulsion is quite similar, showing the absence of any vibrational structure, a broadening of the emission band, and a red shift compared to that in dioxane. The emission band is even more broadened and red-shifted (ca. 15 nm) when CUR is encapsulated in zein NPs and HSA. However, in all cases, the effects observed are less pronounced than those observed in ethanol solution.

This spectroscopic scenario is very similar to that found for CUR either solubilized in dioxane-water mixtures with different water content [21] or encapsulated in surfactant micelles of TX-100 [18]. It indicates that CUR resides in a quite hydrophobic microenvironment but can form intermolecular H-bonds more likely with water molecules at the interface, confined within the host systems, or both. In the case of zein NPs and HSA, the less structured spectral shape and the larger red shift observed in the absorption spectra can also be due to the additional participation of H atoms of the protein scaffolds in intermolecular H-bonds with CUR, according to the well-established binding of CUR with hydrophobic pockets of albumins [29–31]. In these cases, the additional absorption extending beyond 500 nm is reasonably due to a small population of deprotonated CUR as already reported in the literature [18] and, only for zein NPs, also to their typical scattering. Overall, the spectroscopic results suggest that all the investigated hosts shift the tautomeric equilibrium of CUR towards the diketo form, which is present in considerable amounts under these experimental conditions.

Steady-state photolysis experiments were then performed under anaerobic conditions by exciting the host-guest complexes with visible light. The photolysis profile was very similar in all cases, showing a significant bleaching of the main absorption band in the visible region, a slight increase at ca. 330 nm, and a not very clear isosbestic point at ca. 360 nm. This finding accounts for a similar nature of the photodecomposition process. Representative spectral changes observed in the case of CUR encapsulated within Pluronic® _micelles are reported in Fig. 2A. The rate of photobleaching (Fig. 2B), monitored at the maximum absorption of each sample and calculated at the early stage of the photoreactions, was

comparable in the case of polymeric micelles and microemulsions but was significantly smaller (ca. 4–5-fold) in the case of zein NPs and HSA. Note that such a result cannot trivially be attributable to a different amount of photons absorbed by the different samples since, in all cases, the differences in the absorbances at the excitation wavelength are below 5%. The triplet state of any PS is the key intermediate for its photodynamic action. In the case of CUR, the triplet behaviour can be drastically different depending on the predominance of the enolic or diketonic form and the presence of a microenvironment with abstractable H-atom. In their excellent paper, Ortica and Rodgers well highlighted the different triplet dynamics of CUR [21]. They elegantly showed that when CUR is in a solvent with abstractable hydrogens but that does not allow intermolecular H-bonds (i.e., dioxane), leaving the enolic form dominating, it does not behave like a typical carbonyl compound viz hydrogen abstraction by the triplet state. On the other hand, when intermolecular H-bonding to solvent occurs (i.e., adding water to dioxane) and the diketo form is present, CUR behaves like a typical carbonyl compound and hydrogen abstraction by the triplet state takes place from solvents with abstractable H atom (i.e., dioxane or alcohols) [21]. The spectroscopic features illustrated in Fig. 1 and discussed above clearly show that in all the host systems investigated, the diketo form of CUR is clearly present in good amounts. Moreover, all the host systems are rich in many easily abstractable H atoms. Therefore, based on these considerations, we believe that the H-abstraction from the triplet state of CUR may occur in all cases. As illustrated in Scheme 3, the photoreduction process leads to the formation of a ketyl radical as a key intermediate in the CUR photodecomposition (see next section) and subsequent stable photoproducts in which the chromophore conjugation is lost, in agreement with the photobleaching observed. CUR has been extensively proposed as a suitable PS for PDT [7–9]. Here the most active cytotoxic species is the $^1O_2$, formed by collisional energy transfer between the triplet state of the PS and the surrounding molecular oxygen. However, $^1O_2$ generation with acceptable quantum yields Φ_Δ = 0.11, has been reported only in non-polar and not H-bonding solvents [15]. This value drops more than one order of magnitude down in ethanol [15], whereas an average value of Φ_Δ = 0.04 has been recently reported for CUR embedded in liposomes [19]. Thus, we investigated the photogeneration of $^1O_2$ by CUR in the host systems and, for comparison, in dioxane as a reference solvent. The most suitable method to detect $^1O_2$ is direct monitoring by its typical and diagnostic phosphorescence in the near-IR spectral window, which exhibits a maximum at 1270 nm [13]. As shown in Fig. 3, a clear $^1O_2$ signal was detected for CUR dissolved in dioxane, where the enolic form dominates, whereas no detectable $^1O_2$ luminescence was

revealed in any of the host systems. These results suggest that the H-abstraction process is the more likely deactivation pathway of the triplet state of the diketo form and accords well with literature data reporting no formation of $_1O_2$ by CUR encapsulated in different types of micellar systems [15]. The lack of $_1O_2$ photogeneration can also be the result of a lifetime of the CUR triplet lifetime in the hosts short enough to make the diffusional quenching by oxygen not competitive with the triplet decay (see next section).

2.2. Nanosecond Laser Flash Photolysis

Nanosecond laser flash photolysis is a powerful tool for obtaining spectroscopic and kinetic information into photochemically generated transient intermediates. Fig. 4 shows the transient absorption spectra recorded at different delay times after 355 nm pulsed laser excitation of optically matched samples of CUR in dioxane, used as reference solvent, and encapsulated in the various host systems dispersed in water. The spectrum in dioxane (Fig. 4A) shows a broad absorption extending beyond 700 nm, whose decay is not accompanied by the concurrent formation of any further transient. The decay is mono-exponential with a kobs ~ 3.3 × _105 s□ _1 (inset Fig. 4A) and is significantly quenched by oxygen with a quenching constant kq(O2) ~ 1 × _109 M□ _1 s□ _1. According to the literature [20,21], these spectral and kinetic features are unambiguously assigned to the lowest triplet state of CUR, which is exclusively present under the enolic form in this solvent. Furthermore, the relevant quenching by oxygen is in excellent agreement with the observed generation of 1O2 reported in Fig. 3. Interestingly, excitation of CUR in host systems leads in all cases to a transient absorption at the earlier delay time compared with the laser pulse, which is characterized by both a maximum at ca. 490–500 nm and a broad absorption extending in the red region (Fig. 4B-E). These spectral features are very similar to those reported by Ortica and Rodgers for the excitation of CUR in a mixture dioxane water 1:1 (v:v) and assigned by the authors to the ketyl radical produced after H-abstraction by the diketo form, dominant in this solvent mixture, of CUR triplet state from dioxane [21]. Based on these similarities, in our case, the transient observed can be attributed to the ketyl radical generated after H-abstraction by the triplet state of CUR from the host systems that offer several promptly abstractable H atoms. This scenario is in good agreement with the large abundance of the diketo tautomer of CUR demonstrated by the steady-state absorption and emission data, whose presence is indispensable for the H-abstraction to occur (see Fig. 1). The lack of the transient absorption of the triplet state of CUR in the host systems observed at 0.6 μs after the laser pulse accounts for a triplet lifetime shorter than 0.6 μs. This

observation accords very well with the inefficiency of CUR in producing $^1O_2$. In fact, even estimating a diffusion-controlled quenching constant of the triplet state by oxygen (ca. 1×10^9 M^{-1} s^{-1}) and considering an upper limit for the triplet decay of 0.6 μs, the fraction of triplet quenched by oxygen present in solution (ca. 2.6×10^{-4} M) would be about 10%, resulting in an almost complete inefficiency of $^1O_2$ photosensitization. We believe that the short value of the CUR triplet under our experimental conditions can be the result not only of the H-abstraction process but also of the solvent effect of water molecules, inevitably present at the periphery or inside the host systems, on the keto-enolic equilibrium. This hypothesis is in agreement with what already proposed by Ortica and Rodgers, who observed a constant decrease of the triplet lifetime of CUR in dioxane:water mixtures upon increasing the water content up to a limit value below 0.01 μs observed in a 1:1 (v:v) mixture [21]. One interesting aspect to be highlighted is now related to the intensity of the transient absorption of the ketyl radical generated. Inspection of the transient spectra of Fig. 4B-E recorded 0.6 μs after the pulse shows quite similar absorbance values in the case of Pluronic® _micelles and the microemulsion and values ca. 4–5 fold smaller in the case of zein NPs and HSA. Since in all samples, the CUR absorption at the excitation wavelength is very similar, and that relevant differences in the extinction coefficient of the ketyl radical in the different hosts are very unlikely, the differences found in the transient absorption can be reasonably attributed to different amounts of the ketyl radical generated in the different samples. Such differences match very well the rate of the photobleaching observed in the steady-state photolysis experiments reported in Fig. 2B, which showed comparable rates for Pluronic® _micelles and the microemulsion and values ca. 4–5 fold smaller for zein NPs and HSA. This comparison provides strong evidence for the H-abstraction being the main photodeactivation process of the triplet state of CUR encapsulated in the hosts. The different efficiency in photoreactivity can be tentatively attributed to a reduced yield of intersystem crossing (ISC) of CUR in the protein-based hosts. This is not surprising if one considers that the confinement of many drugs in specific hydrophobic pockets with more steric constraints compared with micelles and microemulsions have shown to favour other deactivation pathways from the singlet state competitive with ISC (i.e. fluorescence) [32]. For CUR, this has already been reported when it complexed with albumin [29] and other systems mimicking the hydrophobic pockets of proteins such as cucurbituril [33] and cyclodextrins [34], in which a significant increase of fluorescence has been observed. The decays of the ketyl radical are illustrated in Fig. 5. In all cases, we observed the largest part of the decay being mono-exponential with lifetimes of ca. 7.5 μs in Pluronic® _micelles and

microemulsions (Fig. 5A,B) and ca. 20 μs in Zein NPs and HSA (Fig. 5C,D). The ketyl radical decay is quenched by oxygen (traces b in Fig. 5) unless in zein NPs. The bimolecular constants, kq(O2), were estimated by eq. 1:

$$k_{obs} = k_0 + k_q\,(O2)\,[O2] \qquad (1)$$

where k_{obs} and k0 are the experimental values for the pseudo-first and first-order decay of the ketyl radical observed under air-equilibrated and N2-saturated conditions, respectively, and [O2] is the concentration of oxygen (ca. 2.6×10^{-4} M). We obtained kq(O2) ca. 1×10^{9} M^{-1} s^{-1} in the case of Pluronic® micelles and the microemulsion and ca. 1×10^{8} M^{-1} s^{-1} in the case of HSA. While the latter agrees with those typically expected for a CUR-derived resonance-stabilized carbon centred radical [21,35], the former is quite surprising. We believe that such a quenching constant can be overestimated due to the larger oxygen concentration actually present in the highly hydrophobic environment of the oily phase in microemulsion and polypropylene oxide polymeric chains, which, of course, affects the calculation of kq(O2) by eq. 1. As far as the lack of quenching observed in the case of zein NPs is concerned, this might be the result of the more densely packed structure of this type of NPs compared with HSA, which significantly hinders either access or diffusion of oxygen to the radical centre. Such an effect is not uncommon and has been frequently observed for oxygen-sensitive transient species confined within very restricted microenvironments [32]. Overall, our results demonstrate that in all the host systems, the well-known general mechanism typically observed for the aromatic ketone triplets (i.e., benzophenone) confined in host systems with H-abstractable hydrogens [36–39] may also apply for CUR triplet, as summarized in Scheme 4 and discussed below. H-abstraction by the triplet state of CUR takes place inside the host systems and leads to the formation of triplet radical pairs, the ketyl radical (CURH•), and a host-confined carbon-centered radical (R•). After ISC, they can lead to intra-host covalent recombination products. Besides, the ketyl radical can escape the host destroying the germinate nature of the radical pair. According to the literature, the first-order decay of the ketyl radical observed in our case (kobs) corresponds to the sum of the kISC and kesc processes [38]. This interpretation accords well with the observation that, despite radical-radical combination reactions in homogeneous solutions are usually bimolecular and second-order, these decay processes in confined spaces such as micelles, polymeric matrices, or cyclodextrin cavities are still bimolecular but following first-order kinetics [38–41]. As reported in the seminal papers by Scaiano et al. [38], although the

escape of the ketyl radical destroys the germinate radical pair, it does not destroy the absorption of the ketyl radical chromophore, which, in principle, can be detectable over longer time scales. The kinetic traces observed in our cases show only a small residual absorption after the first-order kinetics were completed. This can be due to either only a small fraction of ketyl radical actually escaped or to a fast formation of decomposition products occurring in the bulk solution. When oxygen is present, the quenching on the ketyl radical decay becomes competitive with the formation of an intra-host recombination product. In our case, reaction with molecular oxygen leads more likely to the formation of the peroxyl radical CURHOO•, which, in principle, may also eliminate the hydroperoxyl radical HOO•, according to what has already been observed for other ketyl radical derivatives [42]. Of course, peroxyl radicals are inevitably formed also through the reaction of oxygen with the host-confined carbon-centred radical R• _which, in contrast to CURH• _has a very low translational mobility.

3. Conclusions and Remarks

The present study provides intriguing insights into the photobehaviour of CUR encapsulated in different host systems such as polymeric micelles, microemulsions, zein NPs, and HSA and further underlines the importance of the microenvironment in dictating the CUR behaviour under light excitation. In all cases, CUR is largely present under the diketo tautomeric form, due to favourable intermolecular H-bonding with water molecules present in the hosts and, in the case of the protein-based systems, probably also with H-bonding protein components. In contrast to the enolic form, the diketo tautomer exhibits the typical reactivity of carbonyl compound viz hydrogen abstraction by the triplet state, leading to the formation of the CUR-derived ketyl radical due to the large presence of easily abstractable H atoms present in the host systems explored. A large part of this radical recombines with the counterpart host-confined radical produced after H-abstraction, generating intra-host covalent products and, in the presence of oxygen, is oxidized by molecular oxygen, generating more likely peroxyl radical species. H-abstraction leads to the loss of the highly conjugated structure of the CUR chromophore, leading to UV-absorbing stable products responsible for the photobleaching observed upon steady-state irradiation. The photobleaching rate is in good agreement with the amount of the ketyl radical detected with time-resolved experiments indicating that the H-abstraction is the primary process responsible for CUR photodecomposition. The triplet state of CUR is short-lived because of a combination of the effective H-abstraction reaction and the solvent effect of water

molecules present in the hosts on the keto-enolic equilibrium. This makes the triplet state quenching by molecular oxygen inefficient, resulting in the lack of $^1O_2$ photogeneration. Taking into account that polymeric micelles, microemulsions, and zein NPs can be considered not only carrier systems to solubilize and deliver CUR but also biological mimicking media, our findings suggest a scenario in which the photodynamic inactivation of bacteria or cancer cells induced by CUR, maybe is not mediated by $^1O_2$, as extensively reported without direct evidence on its photochemical generation. Rather, cytotoxic effects initiated by H-abstraction processes, in which the role of peroxyl radical thereafter formed by the reaction with molecular oxygen can be crucial, need to be considered. The results obtained also deserve some comments regarding the actual view of CUR as PS. Some of the ideal pre-requisites for a good PS include i) strong absorption in the red region, ii) high ISC to triplet and high $^1O_2$ quantum yields, iii) low tendency to auto-oxidation by $^1O_2$ and iv) preferable water solubility [11,12,43]. CUR does not possess any of these features. In fact, it shows i) absorption confined to the not biologically relevant blue spectral window with absorption molar coefficient smaller than those exhibited by typical photosensitizers such as porphyrin and BODIPY derivatives [15]; ii) small, upper limit for ISC and $^1O_2$ quantum yields of ca. 0.1 only in organic solvents such as toluene, benzene and acetonitrile, values that drop significantly down in more polar and H-bonding solvents [16]; iii) high reactivity with $^1O_2$, comparable with that of typical antioxidants [44]; iv) very low solubility in aqueous media. Based on these considerations, we wonder why CUR continues to attract such a wide interest as a PS and if it really deserves such a high reputation and attention from the scientific community. The last aspect we like to highlight is related to using CUR formulations for topical applications as a remedy for preventing and treating skin aging and disorders, which raises serious doubts. Accumulation of CUR in the skin leads to direct absorption of the environmental light and, as recently also emphasized by Becker and coworkers [19], can lead to a more pronounced phototoxic effect when localized in a lipophilic environment. Considering that many formulations possess some features common to those of the carrier systems explored herein, the use of CUR, and the potential of adverse, uncontrolled, and undesired CUR side effects triggered by light on patients cannot be underestimated. Therefore the skin application of CUR is advisable to be avoided, or at least one should pay attention to exposure to environmental light.

4. Experimental Section

4.1. Materials

CUR (C7727, ≥94% curcuminoid content, ≥80% Curcumin), Pluronic® _P123 (EO20–PO70–EO20, MW 5750 g mol□ _1), Pluronic® _F127 (EO100–PO70–EO100, MW 12,600 g mol□ _1), and HSA were purchased from Merck KGaA (Germany). Maize zein (Z) (F4400C non-GMO/food grade) was a kind gift from Flo Chemical Corporation (Ashburnham, MA, USA). Caprylocaproyl macrogol-8 glycerides (Labrasol®) and propylene glycol monolaurate (Lauroglycol 90®) were a kind gift from Gattefoss´e (France). Dioxane and ethanol were purchased from Carlo Erba Reagents and were spectrophotometric grade. Deionized ultra-filtered water was used throughout this study.

4.2. Sample Preparation

4.2.1. Pluronic® Micelles

Empty and loaded micelles were prepared by the thin-film hydration method [29]. Briefly, 100 μL of an ethanolic CUR stock solution (0.2 mg/ mL) and 20 mg of Pluronic® _(10 mg of P123 and 10 mg of F127) were dissolved in absolute ethanol (2 mL) in a round-bottom flask. Then, the solvent was evaporated by rotary evaporation (45 ◦C, 25 min) to obtain a film. The film was left under vacuum overnight to remove residual solvent. After that, the dried film was hydrated with 2 mL of water, and the material was sonicated (10 min), giving a micellar solution. This solution was filtered (0.22 mm filters, RC Chemtek, Italy) to remove the unincorporated drug or possible large cylindrical aggregates formed by P123.

4.2.2. Microemulsion

The microemulsion composition was based on the ternary diagram reported previously by us defining boundaries of the microemulsion domain [28]. CUR was dissolved directly into the Lauroglycol 90®/ Labrasol® _oily phase. A preliminary test was carried out to define the optimal component ratio providing a microemulsion with high curcumin solubilizing capacity and extended colloidal stability. The best-performing prototype was prepared by mixing Lauroglycol 90® _(0.125 mL) and Labrasol® _(1 mL) (300 rpm; 30 min; 40 ◦C) and then adding CUR (0.05 mg from 50 μL of a stock 1 mg/mL in acetone). After that, 5 mL of water were added under magnetic stirring (700 rpm), achieving spontaneous emulsification. The microemulsion was stirred at room temperature for a further 30 min and then left to stabilize for 12 h.

4.2.3. Zein NPs

NPs were fabricated by the modified liquid-liquid dispersion method as previously described [45]. Briefly, Zein (200 mg) was dissolved in ethanol/water 80% *v*/v (10 mL) at room temperature under magnetic stirring. After that, CUR (5 mg) was added to the zein solution until complete solubilization. NPs were formed by adding 50 mL of water to the hydroalcoholic solution under stirring for 15 min and then evaporating ethanol under vacuum. NPs were collected by centrifugation (21,700 *g* for 30 min), washed thrice with water, and stored at 4 °C. *4.2.4. HSA-CUR Complex* 100 µL of an ethanolic CUR stock solution (0.2 mg/mL) was evaporated under vacuum to obtain a thin film. Then, 2 mL of an aqueous solution of $5 \cdot 10^{-5}$ M HSA was added, and the sample stirred for 3 h at room temperature.

4.3. Instrumentations

The average hydrodynamic diameter (D_H) and polydispersity index (PI) were evaluated on a Zetasizer® Nano-ZS (Malvern Instruments, UK). The zeta potential was calculated from the electrophoretic mobility values determined by laser Doppler anemometry (LDA) on the same apparatus. Measurements were performed at a temperature of 25 °C. UV/Vis absorption and fluorescence spectra were recorded in a quartz cell 1.0 cm path length, 3 mL capacity, on a Jasco V-560 spectrophotometer and Fluorolog-2 (Model, F-111) spectrofluorometer, respectively.

4.4. Sample Characterization

4.4.1. Size and Surface Charge

The average hydrodynamic diameter (D_H), polydispersity index (PI), and zeta potential (ζ) of the nanocarriers were determined by Dynamic Light Scattering (DLS) and electrophoretic mobility, respectively. After preparation, Zein NP were diluted 10 folds in Milli-Q water and tested at 25 °C, whereas Pluronic® micelles and the microemulsion were analyzed as such. Results are reported as the mean of three separate measurements on three different batches ± standard deviation (SD).

4.4.2. CUR Content

CUR amount entrapped inside Zein NPs was evaluated by an indirect and a direct method. For the indirect method, NPs were centrifuged (21,700 *g* for 15 min), and the supernatant containing the unloaded drug was collected. An aliquot of supernatant (0.1 mL) was diluted

in ethanol/water 80% *v*/v (1 mL) and analyzed for CUR content. In the direct method, NPs were freeze-dried, an aliquot (*ca.* 8 mg) was treated with 1 mL of ethanol/water at 80% v/v for 1 h, and analyzed for CUR content. CUR amount in the Pluronic® _micelles and microemulsion was The samples were analyzed by UV–vis spectroscopy measuring the absorption at λ _=_ _424 nm using a quartz cell with a 1 cm path length. A calibration curve of CUR in ethanol was built in the concentration range of 0.3–5 μg mL□ _1 (R_2 > 0.99).

4.4.3. Steady-State Photolysis

Irradiation of the samples was performed in a thermostated quartz cell (1 cm path length, 3 mL capacity, 25 ◦C) by using a 100 mW continuum laser with λ_{exc} =_ _405 nm after purging the sample solutions with a flux of N_2 for 20 min.

4.4.4. Laser Flash Photolysis

All of the samples were excited with the third harmonic of Nd–YAG Continuum Surelite II–10 laser (355 nm, 6 ns FWHM), using quartz cells with a path length of 1.0 cm. The excited solutions were analyzed with a Luzchem Research mLFP–111 apparatus with an orthogonal pump/ probe configuration. The probe source was a ceramic xenon lamp coupled to quartz fibre-optic cables. The laser pulse and the mLFP–111 system were synchronized by a Tektronix TDS 3032 digitizer, operating in pre-trigger mode. The signals from a compact Hamamatsu photomultiplier were initially captured by the digitizer and then transferred to a personal computer, controlled by Luzchem Research software operating in the National Instruments LabView 5.1 environment. The solutions were deoxygenated *via* bubbling with a vigorous and constant flux of pure nitrogen (previously saturated with solvent). In all of these experiments, the solutions were renewed after each laser shot (in a flow cell of 1 cm optical path), to prevent sample photodegradation. The sample temperature was 295 ± _2 K. The energy of the laser pulse was measured at each shot with a SPHD25 Scientech pyroelectric meter.

4.4.5. Singlet Oxygen Detection

The NIR luminescence of $^1O_2$ at 1.27 μm results from the forbidden transition $^3\Sigma_g$□ _← _$^1\Delta_g$. This steady-state emission was registered with the same spectrofluorimeter as above equipped with a NIR-sensitive liquid nitrogen cooled photomultiplier, exciting the air-equilibrated samples with a 405 nm continuum laser (100 mW).

5. Declaration of Competing Interest

No competing interest to declare.

6. Data availability

Data will be made available on request.

7. Acknowledgments

We thank the PhotoNCur - PIAno di incentivi per la RIcerca di Ateneo 2020-2022 linea 3 “starting grant” _and the Programma Operativo Nazionale Ricerca e Innovazione 2014-2020 (CCI 2014IT16M2OP005) Fondo Sociale Europeo, Azione I.1 “Dottorati Innovativi con Caratterizzazione Industriale”.

8. References

[1] V. Sueth-Santiago, G.P. Mendes-Silva, D. Decote-Ricardo, M.E.F. de Lima, Curcumin, the golden powder from turmeric: insights into chemical and biological activities, Quim Nova 38 (4) (2015) 538–552.

[2] M. Salem, S. Rohani, E.R. Gillies, Curcumin, a promising anticancer therapeutic: a review of its chemical properties, bioactivity and approaches to cancer cell delivery, RSC Adv. 4 (2014) 10815–10829.

[3] M.J. Dehzad, H. Ghalandari, M. Nouri, M. Askarpour, Antioxidant and anti-inflammatory effects of curcumin/turmeric supplementation in adults: a grade-assessed systematic review and dose–response meta-analysis of randomized controlled trials, Cytokine 164 (2023) 156144–156162.

[4] Dania Akbik, Maliheh Ghadiri, W. Chrzanowski, Ramin Rohanizadeh, Curcumin as a wound healing agent, Life Sci. 116 (2014) 1–7.

[5] A.M. Pourbagher-Shahri, T. Farkhondeh, M. Ashrafizadeh, M. Talebi, S. Samargahndian, Curcumin and cardiovascular diseases: focus on cellular targets and cascades, Biomed. Pharmacother. 136 (2021) 111214–111230.

[6] S. Mukherjee, A.K. Mishra, G.D.G. Peer, S.A. Bagabir, S. Haque, R.P. Pandey, V. S. Raj, N. Jain, A. Pandey, S.K. Kar, The interplay of the unfolded protein response in

517 neurodegenerative diseases: a therapeutic role of curcumin, Front. Aging Neurosci. 13
518 (2021) 767493–767502.
519 [7] K.T. Kazantzis, K. Koutsonikoli, B. Mavroidi, M. Zachariadis, P. Alexiou, M. Pelecanou,
520 K. Politopoulos, E. Alexandratou, M. Sagnou, Curcumin derivatives as photosensitizers in
521 photodynamic therapy: photophysical properties and in vitro studies with prostate cancer
522 cells, Photochem. Photobiol. Sci. 19 (2020) 193–206.
523 [8] C. Santezi, B.D. Reina, L.N. Dovigo, Curcumin-mediated photodynamic therapy for the
524 treatment of oral infections - A review, photodiagnosis and photodynamic therapy 21, 2018,
525 pp. 409–415.
526 [9] L.D. Dias, K.C. Blanco, I.S. Mfouo-Tynga, N.M. Inada, V.S. Bagnato, Curcumin as a
527 photosensitizer: from molecular structure to recent advances in antimicrobial photodynamic
528 therapy, J Photochem Photobiol C: Photochem Rev 45 (2020) 100384–100418.
529 [10] P. Agostinis, K. Berg, K.A. Cengel, T.H. Foster, A.W. Girotti, S.O. Gollnick, S. M. Hahn,
530 M.R. Hamblin, A. Juzeniene, D. Kessel, M. Korbelik, J. Moan, P. Mroz, D. Nowis, J. Piette,
531 B.C. Wilson, J. Golab, Photodynamic therapy of cancer: an update, Ca-Cancer J. Clin. 61
532 (2011) 250–281.
533 [11] M.R. Hamblin, T. Hasan, Photodynamic therapy: a new antimicrobial approach to
534 infectious disease? Photochem. Photobiol. Sci. 3 (2004) 436–450.
535 [12] J.P. Celli, B.Q. Spring, I. Rizvi, C.L. Evans, K.S. Samkoe, S. Verma, B.W. Pogue, T.
536 Hasan, Imaging and photodynamic therapy: mechanisms, monitoring, and optimization,
537 Chem. Rev. 110 (2010) 2795–2838.
538 [13] P.R. Ogilby, Singlet oxygen: there is indeed something new under the sun, Chem. Soc.
539 Rev. 39 (2010) 3181–3209.
540 [14] K.I. Priyadarsini, Photophysics, photochemistry and photobiology of curcumin: studies
541 from organic solutions, bio-mimetics and living cells, J Photochem Photobiol C: Photochem
542 Rev 10 (2009) 81–95.
543 [15] C.F. Chignell, P. Bilski, K.J. Reszka, A.N. Motten, R.H. Sik, T.A. Dhal, Spectral and
544 photochemical properties of curcumin, Photochem. Photobiol. 59 (1994) 295–302.
545 [16] S.M. Khopde, K.I. Priyadarsini, D.K. Palit, T. Mukherjee, Effect of solvent on the excited-
546 state photophysical properties of curcumin, Photochem. Photobiol. 72 (2000) 625–631.
547 [17] L. Nardo, R. Paderno, A. Andreoni, M. M´asson, T. Haukvik, H.H. Tønnesen, Role of H-
548 bond formation in the photoreactivity of curcumin, Spectroscopy 22 (2008) 187–198.

549 [18] R. Adhikary, P.J. Carlson, T.W. Kee, J.W. Petrich, Excited-state intramolecular
550 hydrogen atom transfer of curcumin in surfactant micelles, J. Phys. Chem. B 114 (2010)
551 2997–3004.
552 [19] A. Wolnicka-Glubisz, M. Olchawa, M. Duda, P. Pabisz, A. Wisniewska-Becker, The role
553 of singlet oxygen in photoreactivity and phototoxicity of curcumin, Photochem. Photobiol. 99
554 (2023) 57–67.
555 [20] A.A. Gorman, I. Hamblett, V.S. Srinavasan, P.D. Wood, Photochem. Photobiol. 59
556 (1994) 389–398.
557 [21] F. Ortica, M.A.J. Rodgers, A laser flash photolysis study of curcumin in dioxane-water
558 mixtures, Photochem. Photobiol. 74 (2001) 745–751.
559 [22] H.H. Tønnesen, A.F. Arrieta, D. Lerner, Studies on curcumin and curcuminoids. Part
560 XXIV: characterization of the spectroscopic properties of the naturally occurring
561 curcuminoids and selected derivatives, Pharmazie 50 (1995) 689–693.
562 [23] R. Tabanelli, S. Brogi, V. Calderone, Improving curcumin bioavailability: current
563 strategies and future perspectives, Pharmaceutics 13 (2021) 1715–1751.
564 [24] S. Maleki, D.M. Alipour, E.D. Abdolahinia, E. Ahmadian, A. Eftekhari, H. Forouhandeh,
565 Y.R. Saadat, S. Sharifi, S.Z. Vahed, Curcumin nanoformulations: beneficial nanomedicine
566 against cancer, Phytother. Res. 36 (2022) 1156–1181.
567 [25] A. Karthikeyan, N. Senthil, T. Min, Nanocurcumin: a promising candidate for therapeutic
568 applications, Front. Pharmacol. 11 (2020) 487.
569 [26] M.A. T˘anase, A.C. Soare, L.M. Ditu, C.L. Nistor, C.I. Mihaescu, I.C. Gifu, C. Petcu, L.
570 O. Cinteza, Influence of the hydrophobicity of pluronic micelles encapsulating curcumin on
571 the membrane permeability and enhancement of photoinduced antibacterial, Pharmaceutics
572 14 (2022) 2137.
573 [27] C.-H. Liu, W.-S. Lee, W.-C. Wu, Photodynamic inactivation against Pseudomonas
574 aeruginosa by curcumin microemulsions, RSC Adv. 6 (2016) 63013–63022.
575 [28] A. Fraix, O. Catanzano, I. Di Bari, C. Conte, M. Seggio, C. Parisi, A. Nostro, G. Ginestra,
576 F. Quaglia, S. Sortino, Visible light-activatable multicargo microemulsions with bimodal
577 photobactericidal action and dual colour fluorescence, J. Mater. Chem. B 7 (2019) 5257–
578 5264.
579 [29] A. Barik, K.I. Priyadarsini, H. Mohan, Photophysical studies on binding of curcumin to
580 bovine serum albumin, Photochem. Photobiol. 77 (2003) 597–603.

581 [30] H. Dezhampanah, Z. Shabanzade, Investigation of binding interaction between human
582 serum albuminwith zirconium complex of curcumin and curcumin, J. Biomol. Struct. Dynam.
583 40 (2022) 722–732.
584 [31] A.C.P. Reddy, E. Sudharshan, A.G. Appu Rao, B.R. Lokesh, Interaction of curcumin
585 with human serum albumin-a spectroscopic study, Lipids 34 (1999) 1025–1029.
586 [32] S. Monti, S. Sortino, Photoprocesses of non-steroidal anti-inflammatory drugs within
587 cyclodextrin cavities, Chem. Soc. Rev. 31 (2002) 287–300.
588 [33] M.A. Rankin, B.D. Wagners, Fluorescence enhancement of curcumin upon inclusion
589 into cucurbituril, Supramol. Chem. 16 (2004) 513–519.
590 [34] K.N. Bagole, P.G. Boland, B.D. Wagner, Fluorescence enhancement of curcumin upon
591 inclusion into parent and modified cyclodextrins, J. Photochem. Photobiol. A Chem. 173
592 (2005) 230–237.
593 [35] S.V. Jovanovic, C.W. Boone, S. Steenken, M. Trinoga, R.B. Kaskey, How curcumin
594 works preferentially with water soluble antioxidants, J. Am. Chem. Soc. 123 (2001) 3064–
595 3068.
596 [36] N.J. Turro, V. Ramamurthy, J.C. Scaiano, Modern Molecular Photochemistry of Organic
597 Molecules, University Science Books, Sausalito, CA, 2010.
598 [37] J.C. Scaiano, C. Selwyn, Dynamic aspects of the behavior of aromatic ketone triplets
599 in anionic micelles. A laser flash photolysis study, Can. J. Chem. 59 (1981) 2368–2372.
600 [38] J.C. Scaiano, E.B. Abuin, L.C. Stewart, Photochemistry of benzophenone in micelles.
601 Formation and decay of radical pairs, J. Am. Chem. Soc. 104 (1982) 5673–5679.
602 [39] P.P. Levin, A.F. Efremkin, N.B. Sultimova, V.V. Kasparov, I.V. Khudyakov, Decay
603 kinetics of benzophenone triplets and corresponding free radicals in soft and rigid polymers
604 studied by laser flash photolysis, Photochem. Photobiol. 90 (2014) 369–373.
605 [40] P. Bortolus, S. Monti, Photochemistry in cyclodextrin cavities, Adv. Photochem. 21
606 (1996) 1–133.
607 [41] M.D. Hatlee, J.J. Kozak, G. Rothenberger, P.P. Infelta, M. Gr´atzel, Role of
608 dimensionality and spatial extent in influencing intramicellar kinetic processes, J. Phys.
609 Chem. 84 (1980) 1508–1519.
610 [42] C. Fabbri, M. Bietti, O. Lanzalunga, Reactivity of ketyl radicals with lignin related
611 structures. On the importance of the ketyl pathway in the photoyellowing of lignin containing
612 pulps and papers, J. Organomet. Chem. 70 (2005) 2720–2728.

613 [43] M. Wainmwright, Photosensitizers in Biomedicine, Wiley-Blackwell, 2009. [44] K.C.
614 Das, C.K. Das, Curcumin (diferuloylmethane), a singlet oxygen ($_1O_2$) quencher, Biochem.
615 Biophys. Res. Commun. 295 (2002) 62–66.
616 [45] D. Esposito, C. Conte, I. D'Angelo, A. Miro, F. Ungaro, F. Quaglia, Mucoadhesive
617 zein/beta-cyclodextrin nanoparticles for the buccal delivery of curcumin, Int. J. Pharm. 586
618 (2020) 119587–119593.

Figures

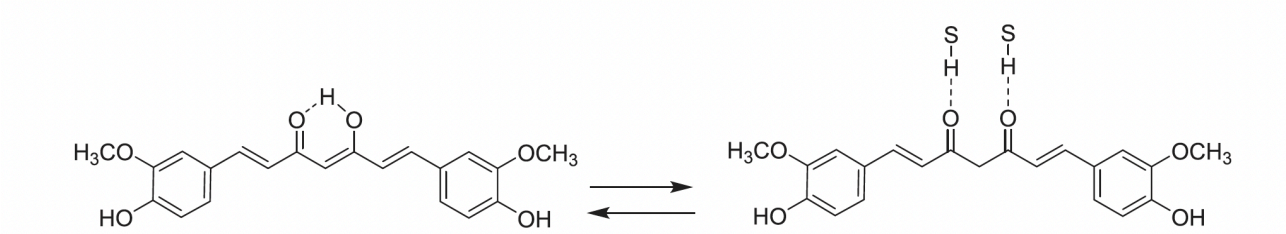

Scheme 1. The equilibrium between the enolic (left) and diketo (right) forms of CUR. The latter dominates in the presence of H-bond donating solvents/substrates (SH).

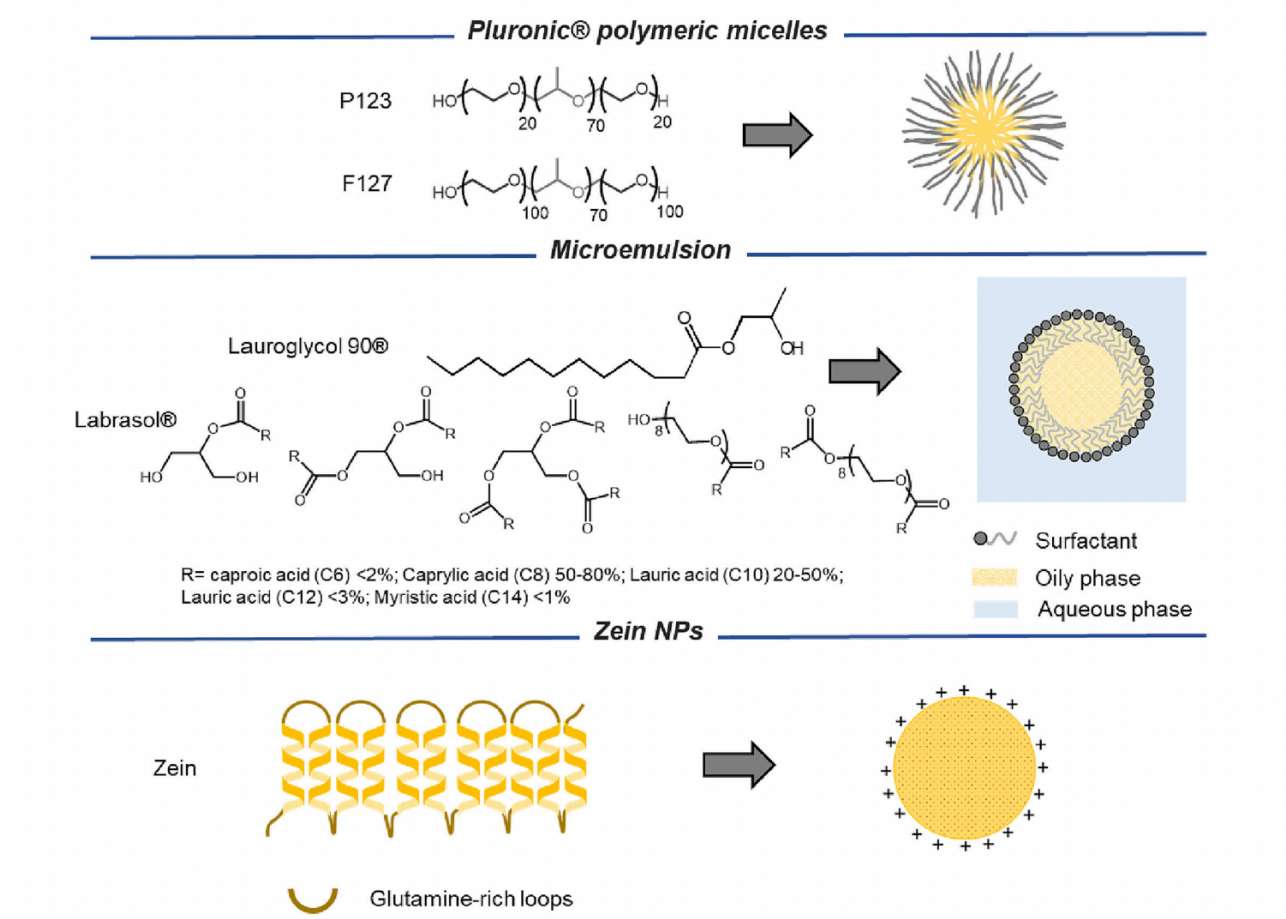

Scheme 2. Schematic of the biocompatible nanocarriers used in this work and molecular structures of their components.

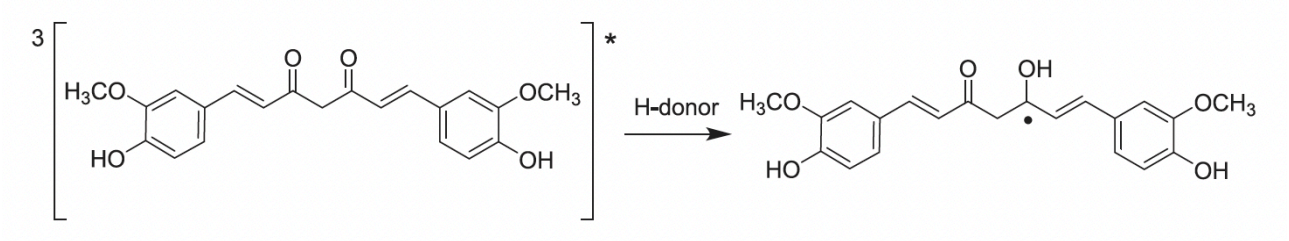

Scheme 3. Hydrogen abstraction from the host systems by the triplet state of the diketo form of CUR leading to the generation of a ketyl radical.

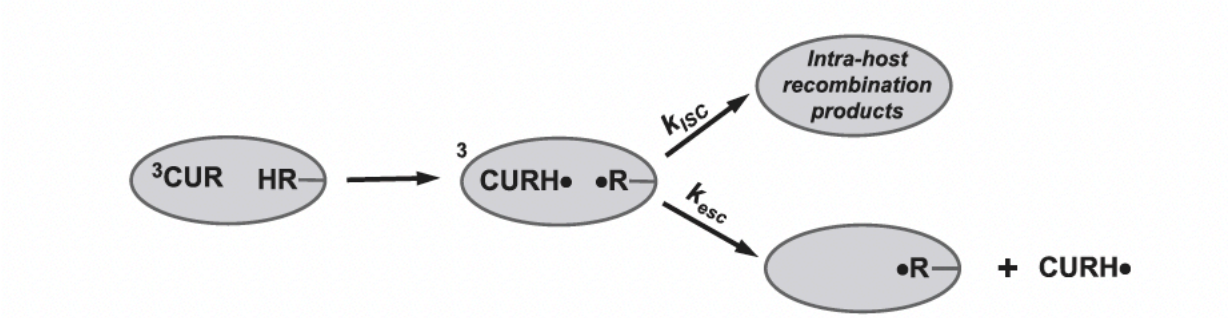

Scheme 4. Primary photochemical processes of CUR in the host systems investigated. R is the host component with abstractable H atoms.

Table 1 Properties of CUR-loaded nanocarriers. Results are reported as the mean of three separate measurements on three different batches ± _standard deviation (SD).

Nanocarriers	D_H (nm)	PI	ζ (mV)	CUR[a] (μg mL^{-1})
Pluronic® micelles	28 ± 2.3	0.198 ± 0.05	−0.7 ± 0.9	10
Microemulsion	29 ± 0.2	0.264 ± 0.02	−0.1 ± 0.6	10
Zein NPs	124 ± 11	0.174 ± 0.07	+48 ± 3	82[b]

CUR concentration in the as prepared samples. [b]Evaluated by the direct and indirect method as specified in 4.3. SD of CUR amount was 82 ± _1 μg mL□ _1

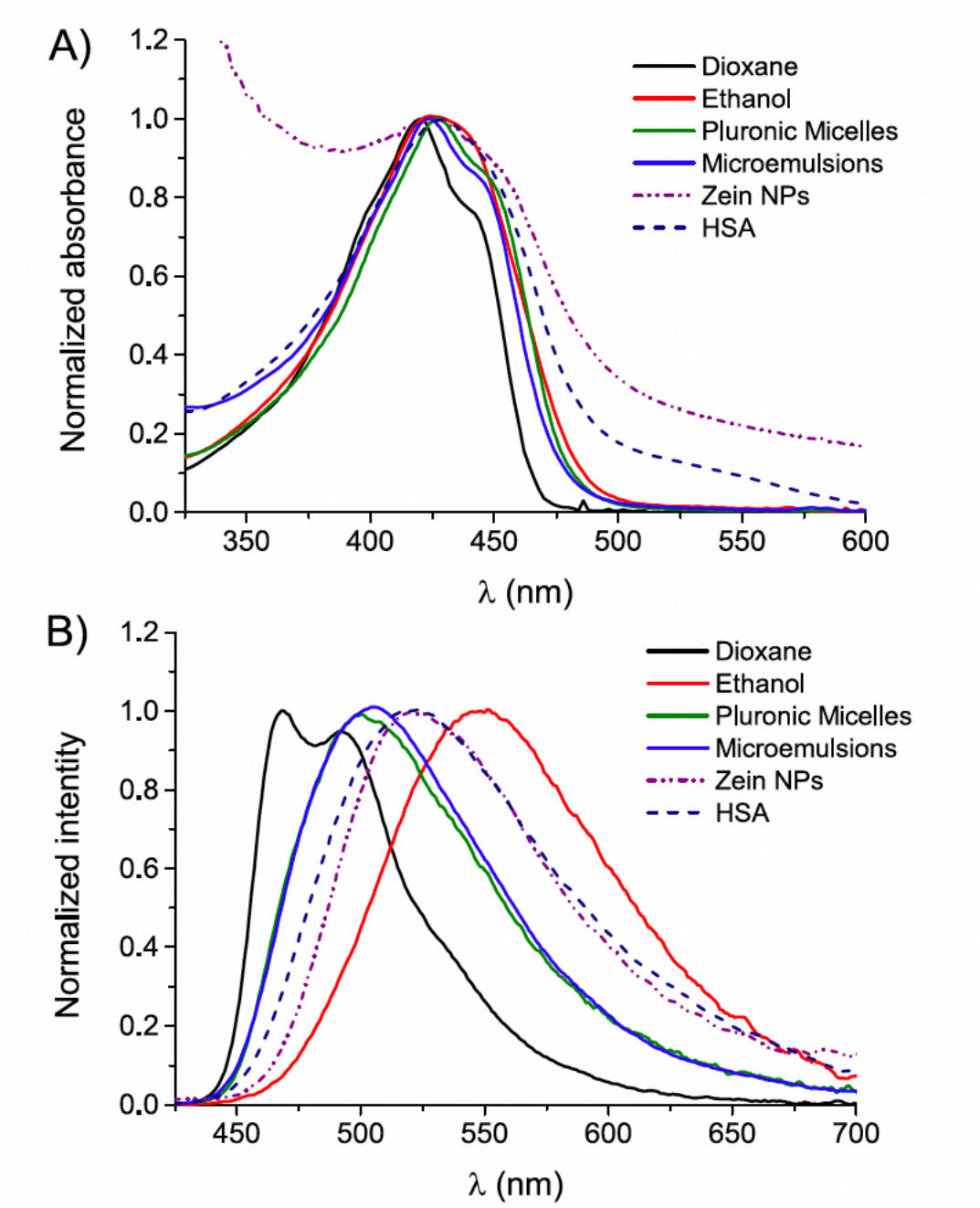

Fig. 1. Normalized (A) absorption and (B) fluorescence emission (λ_{exc} =_ _400 nm) spectra of CUR in different solvents and host systems. *T* =_ _25 °C..

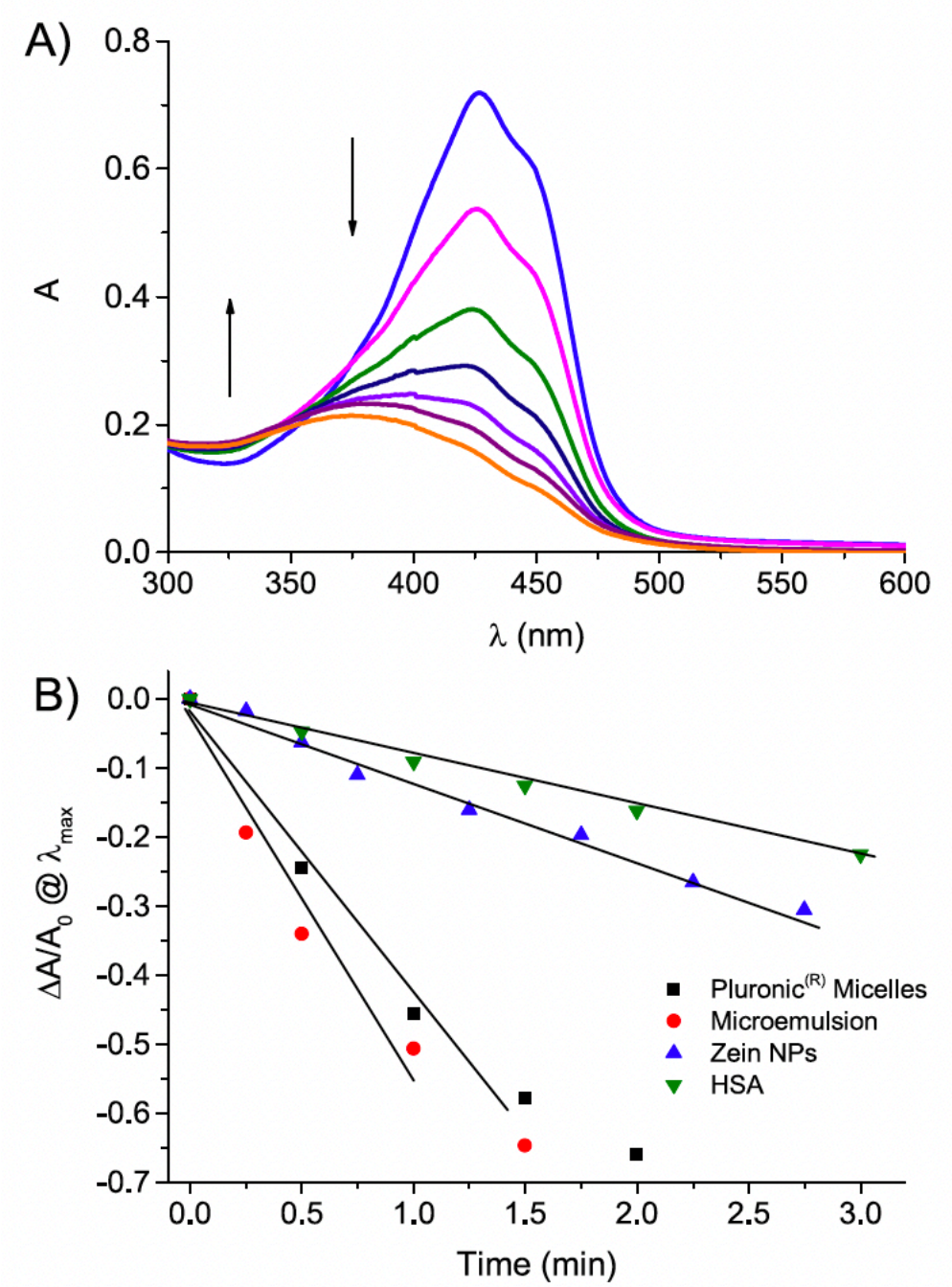

Fig. 2. (A) Representative absorption spectral changes observed upon exposure of a N_2-saturated aqueous solution of CUR (10 μg mL^{-1}) loaded in Pluronic® micelles at λ_{exc} = 405 nm (ca. 100 mW cm^{-2}) for time intervals from 0 to 3 min. The arrows indicate the course of the spectral profile with the illumination time. T = 25 °C. (B) Absorbance differences over initial absorbance as a function of the irradiation time for CUR encapsulated in different host systems. The continuous lines show the linear plot of the photobleaching rate calculated at the early stage of the photoreactions.

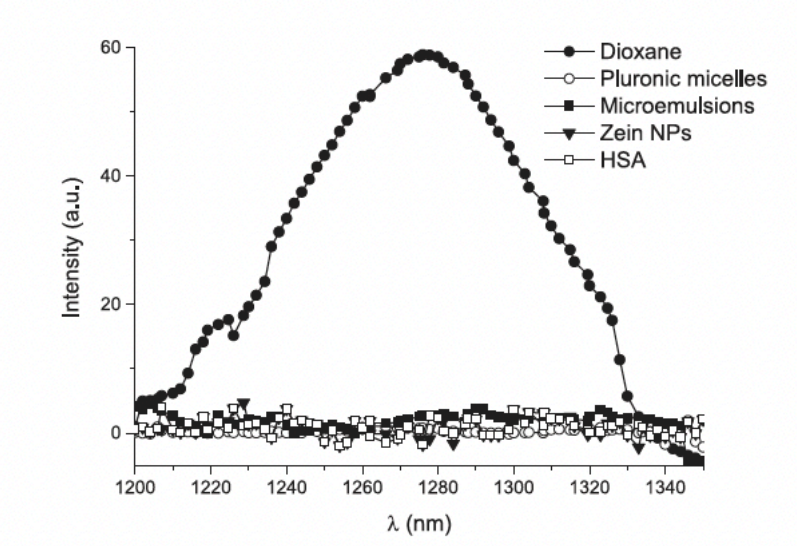

Fig. 3. $^1O_2$ luminescence detected upon 405 nm light excitation of solutions of CUR (10 μg mL^{-1}) in dioxane and host systems in D_2O. *T* = 25 °C.

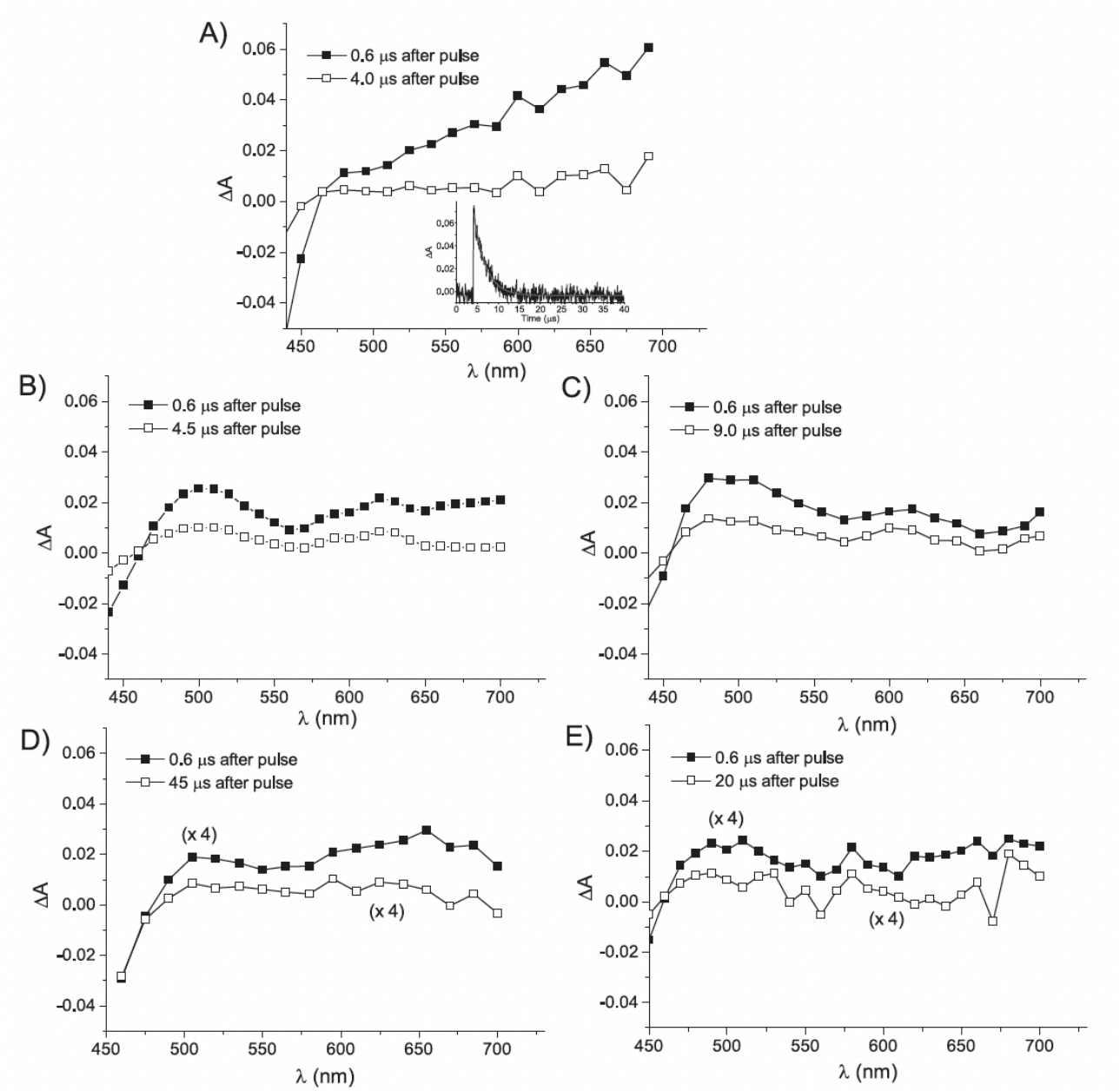

Fig. 4. Transient absorption spectra obtained upon 355 nm laser excitation (E_{355} 10 mJ pulse^{-1}) of optically matched N_2-saturated samples of CUR (A_{355} ~ 0.3) and recorded at different delay times of the laser pulse. CUR in dioxane; the inset shows the decay trace and the related first-order fitting monitored at 700 nm (A). CUR in Pluronic® _micelles (B), the microemulsion (C), zein NPs (D) and HSA (E). For clarity, the spectra of samples (D) and (E) have been multiplied by a factor 4.

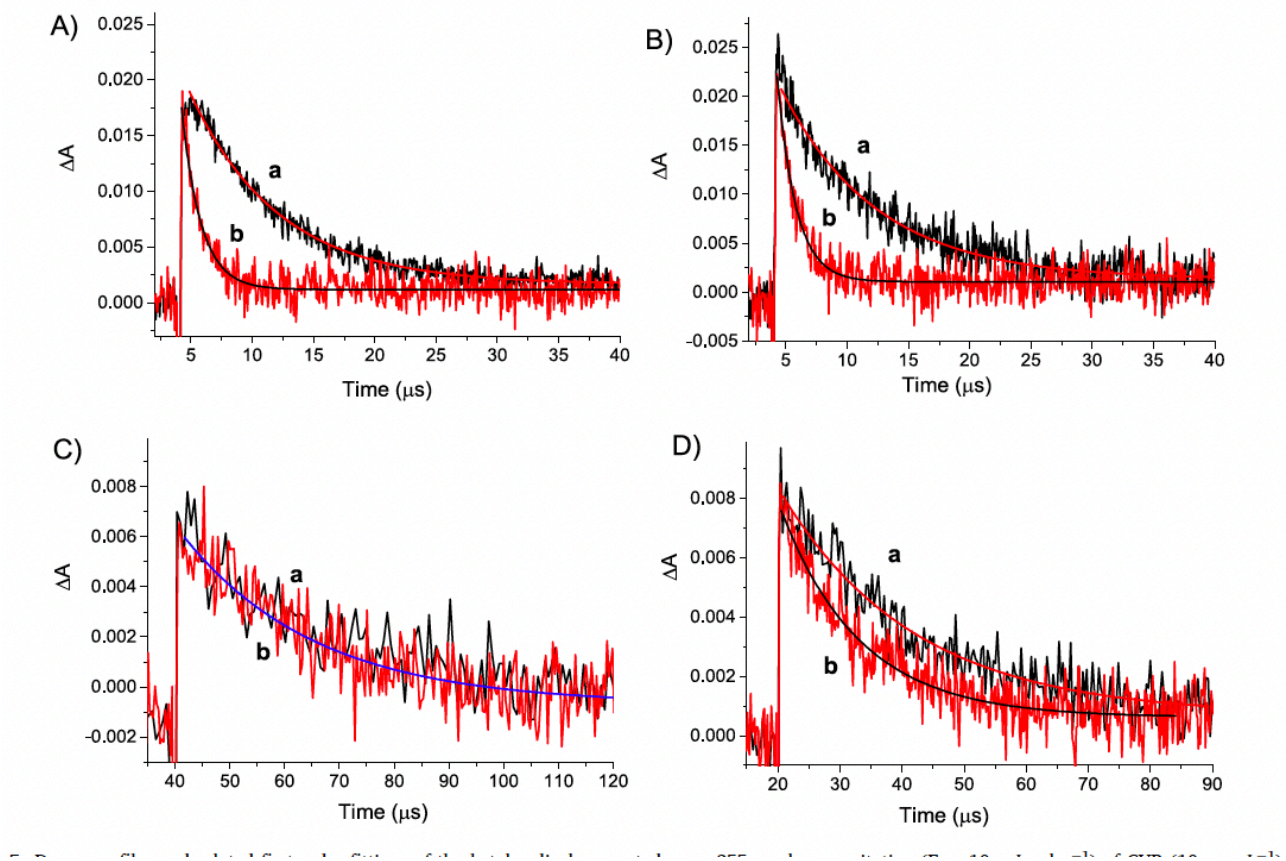

Fig. 5. Decay profiles and related first-order fittings of the ketyl radical generated upon 355 nm laser excitation (E_{355} 10 mJ pulse^{-1}) of CUR (10 μg mL^{-1}) in Pluronic® micelles (A), the microemulsion (B), zein NPs (C) and HSA (D) and recorded in N_2-saturated (**a**) and air-equilibrated conditions (**b**).